Rehydration of food powders: interplay between physical properties and process conditions

Ong, X.Y., Taylor, S.E. and Ramaioli, M.

Rehydration of Food Powders: Interplay Between Physical Properties and Process Conditions

Xin Yi Ong[a,b,*], *Spencer E. Taylor*[c], *Marco Ramaioli*[a,d]

[a] Department of Chemical and Process Engineering, University of Surrey, GU2 7XH, United Kingdom.

[b] School of Engineering, Technology and Design, Canterbury Christ Church University, Canterbury, Kent, CT1 1QU, United Kingdom.

[c] Department of Chemistry, University of Surrey, GU2 7XH, United Kingdom.

[d] UMR 782, GMPA, INRA, 78850 France.

Food powders, powder rehydration, dissolution, lump formation

ABSTRACT: Dehydrated food powders with poor dissolution or dispersion can dramatically compromise food processing, with consequences for the final product quality and consumer experience. In this study, the reconstitution performance of maltodextrin powders with different

moisture content and molecular weight, has been determined by varying the processing conditions, including agitation speed, liquid temperature, powder addition rate and mode of addition to the liquid surface.

In particular, the inter-relationship between the glass transition temperature (T_g) of the powder, its moisture content and the liquid temperature (T_L) is highlighted. When $T_L \geq T_g$, the individual maltodextrin granules tend to swell, restricting further dispersion and rehydration. It has been shown that higher liquid temperatures reduce the dispersion of food powders containing high molecular weight carbohydrates. Increasing the rate of powder addition to the liquid surface under low agitation conditions has been shown to result in faster reconstitution of low-molecular weight maltodextrins, whilst, on the other hand, the corresponding reconstitution rates of high-molecular weight maltodextrins are reduced.

On the basis of this work and a previous study [X.Y. Ong, S.E. Taylor and M. Ramaioli, Pouring of Grains onto Liquid Surfaces: Dispersion or Lump Formation? *Langmuir* (2019) 11150-11156] an improved, yet simple, approach to improve powder dispersion in a liquid is also demonstrated, by optimizing the distribution of the powder on the liquid surface. This approach avoids powder grains accumulating as heterogeneous lumps on the liquid surface and has been applied herein to a wide range of food powders.

1. INTRODUCTION

The dispersion of a powder in a liquid has received a lot of interest both theoretically and empirically. This process is relevant to many industries, including food, pharmaceuticals, paint and detergent sectors. According to Crowley et al. [1], the process of dispersing powders in liquids

can be divided into four distinct stages: wetting, capillarity, dispersion and dissolution. Minor changes in the physicochemical properties of the powder can potentially affect the progression of these stages. Undesirable heterogeneous lumps are recurrent in many industrial processes and the conditions leading to their formation have been recently elaborated for insoluble grains [2,3]. According to Ong et al. [3], the conditions under which grain dispersion or lump formation occurs can be identified based on the contact angle, Bond number and the density ratio, D (also known as the ratio of the weight of a grain to the maximum buoyancy force).

The wetting and reconstitution of soluble food powders is more complex than for insoluble powders [4]. In the case of amorphous polysaccharides, for example, wetting is greatly influenced by the water sorption isotherm [5], diffusion of the water into the amorphous polysaccharide grains [6,7], and viscous effects [8,9]. In these systems, there are also two intermediate steps in the rehydration process involving capillarity and dispersion.

Several studies have shown that poor water dispersion can lead to the formation of lumps with maltodextrin powders [4,10–16]. Indeed, due to their wetting and dispersion properties, aggregation occurs at the same time as the dissolution and diffusion of water within the bulk grains [17]. A gel phase has also been observed to form during swelling [6].

In the present work, we consider the interplay that the maltodextrin properties of moisture content and molecular weight, and the process conditions of agitation speed, liquid temperature and powder addition rate, have on the reconstitution kinetics. On the basis of the present findings, together with those of a previous study [3], a novel, yet simple, powder distribution approach has demonstrated a significant improvement to the dispersion and dissolution of some food powders.

2. EXPERIMENTAL

2.1 Materials

Food powders often contain many ingredients, including additives, such as surfactants. Maltodextrins are carbohydrates that are commonly used in dehydrated food beverages as bland-tasting fillers and thickeners. Another complex powder that is often used as an emulsifier and stabilizer in dehydrated food beverages is milk protein, which contains different proportions of caseins, whey proteins, lactose, fats, minerals and vitamins [18]. Literature reports indicate that these ingredients have very poor wettability and are difficult to disperse in water [4,12,16,19,20]. In the present work, the following four food powders containing the above components were selected for study:

- Maltodextrins DE2 ($M_w \approx 343{,}000$ g mol^{-1}) and DE21 ($M_w \approx 7260$ g mol^{-1}) from Roquette (France);
- Whole fat milk powder (WMP) from Dairygold Food Ingredients(Ireland);
- "Horlicks" commercial cocoa malted beverage produced by Aimia Foods (UK).

A single batch of each powder was used throughout the experiments. These were stored in sealed aluminum bags in a controlled temperature environment (22 °C) to avoid changes to the physical and chemical properties prior to conducting the experiments. "Evian" mineral water was used as the dissolution medium throughout.

Maltodextrins are polysaccharides consisting of a large number of glucose monosaccharide units connected through glycoside bonds. They are typically classified in terms of their dextrose equivalent (*DE*), which indicates the content of reducing sugars. The *DE* value is inversely related to the length of the polysaccharide chain, and thus its molecular weight [21].

The particle size distributions of the powders were measured using a QICPIC particle size analyzer, based on image analysis (Sympatec GmbH, Clausthal-Zellerfeld, Germany). d_{10}, d_{50} and d_{90}, the diameters corresponding to 10, 50 and 90% of the volume of particles in the distribution,

were determined and used to calculate the span (s) of the distributions, defined as $s = (d_{90} - d_{10}) / d_{50}$, which provides a measure of the distribution width. The apparent particle density was measured by gas pycnometry (AccuPycnometer 1330, Micrometrics Instrument Corp., Norcross, GA, USA). Poured bulk density was measured by weighing known powder volumes in graduated cylinders. Table 1 summarizes the size and density characteristics of the different powders used in this study. The instantaneous (determined after 1 s) grain contact angles given in Table 1 are literature values [4,12], determined using the sessile drop method.

Table 1: Properties of the powders used in this study

Powder	d_{50} (μm)	Span, s	Apparent density (kg/m^3)	Poured bulk density (kg/m^3)	Contact angle at t = 1 s (°)
DE 2	161	1.32	1498	503	> 46 (from DE6) [12]
DE 21	179	1.39	1496	515	24 [12]
WMP	315	2.15	1253	378	104 [4]
Horlicks	290	1.87	1317	516	-

In order to modify water activity (a_w), powder samples were equilibrated on shelves inside a controlled humidity chamber (MMM Climacell 111 ECO Environmental Test Chamber, UK) for two weeks. The powders were spread thinly to a depth of approximately 5 mm to increase the surface area for water absorption, which was monitored with an HD1 Thermo Hygrometer (Rotronic, Switzerland).

The chamber temperature was maintained constant at 22 ℃ and the relative humidity (RH) was adjusted to 30, 40 and 50%. The humidity chamber can contain relatively large quantities of powders, and there is a continuous humidified air circulation with a ventilator that leads to faster moisture absorption and equilibration [22]. Owing to limitations of the chamber, equilibration at

the lowest *RH* (22%) was achieved by storing powders in desiccators at 22 °C over saturated potassium acetate CH_3COOK (Sigma-Aldrich Ltd.) solution.

The moisture contents of powders that were conditioned as described above were measured gravimetrically using an OHAUS MB35 Moisture Analyser. The average moisture contents of triplicate samples are given in Table 2. Glass transition temperatures T_g were measured by differential scanning calorimetry Q2000 (TA Instruments, United States). T_g was determined from the onset temperature of inflection occurring in the heat flow curve.

Table 2: Preparation method (storage conditions), moisture content (%), T_g and a_w at 22 °C for the powders studied.

Powder	Storage conditions	Moisture content (%)	T_g (°C)	a_w
DE2	-	6.9	87.3	0.26
DE2	Desiccator with saturated CH_3COOK solution (30 days)	6.5	93.2	0.22
DE2	Chamber (14 days), *RH* = 30%	8.6	77.3	0.33
DE2	Chamber (14 days), *RH* = 40%	9.2	60.9	0.43
DE2	Chamber (14 days), *RH* = 50%	10.5	48.6	0.49
DE21	-	4.0	72.3	0.30
DE21	Desiccator with saturated CH_3COOK solution (30 days)	3.7	74.6	0.22
DE21	Chamber (14 days), *RH* = 30%	4.4	73.0	0.33
DE21	Chamber (14 days), *RH* = 40%	5.9	63.9	0.43
DE21	Chamber (14 days), *RH* = 50%	7.1	60.6	0.49
WMP	-	3.9	-	-
Horlicks	-	3.8	-	-

2.2 Methods

Two different sizes of double-jacketed dissolution vessel were used to explore the dispersion and dissolution of food powders. The dimensions of both vessels and the magnetic stirrers used in both vessels are given in Table 3.

Table 3: Dimensions of the dissolution vessels. The amounts of powder and water used in each system to reach a final concentration of 7.41 wt% are given.

Vessel	Height of liquid H_L (cm)	Diameter D_T (cm)	Cross sectional area (cm^2)	Aspect ratio (D_T /H_L)	Amount of powder (g)	Amount of water (mL)	Stirrer (mm)
Small	4.0	6.0	28.3	1.50	12.8	160	30 × 8
Large	8.5	8.5	56.7	1.00	40	500	45 × 8

The dissolution kinetics of the powders were determined by means of a refractive index sensor (FISO FTI-10, Single Channel Signal Conditioner; FISO Technologies Inc., Quebec, Canada), and a conductivity probe (FiveEasy™ F30 Conductivity Meters, Mettler-Toledo, UK). Powders containing electrolytes (WMP and Horlicks) increased the conductivity of the liquid medium during dissolution, whereas non-conducting materials (DE21 and DE2) caused a decrease. As shown in Figure 1, the refractive index sensor and conductivity probe were set into the double-jacketed vessel which is connected to an external water bath in order to control the temperature of the contents. Refractive index and conductivity data were recorded every 1 s for 5 minutes and normalised using the following equation:

$$DI(t) = \frac{X(t) - X(t_o)}{X(\infty) - X(t_o)} \quad (1)$$

where *DI(t)* is the normalized dissolution index, *X(t)* is the reading at time t, $X(t_o)$ is the initial reading for water and $X(\infty)$ is the final reading after complete dissolution of the powder.

In some experiments, complete dissolution of the powder was not achievable after five minutes, hence $X(\infty)$ was subsequently obtained by manually stirring the solution until all the powder was fully dissolved, and a clear solution was obtained.

A typical comparison between the normalized conductivity and refractive index readings is shown in Appendix A. The results are seen to be comparable and this suggests that both conductivity and refractive index are responding consistently to the dissolution processes and could therefore be used to compare the dissolution behaviour of the powders. Additionally, given that the probes are located opposite to each another in the vessel, the very similar behavior seen

confirms that good mixing is being achieved within the cell, even at the lowest agitation speed of 100 rpm. However, the individual readings from the refractive index probe were found to be generally subject to much larger fluctuations, leading to a greater level of noise in the data. Hence, refractive index will not be used in this study. Accordingly, visual assessment and conductivity measurements form the basis of the subsequent discussions presented herein.

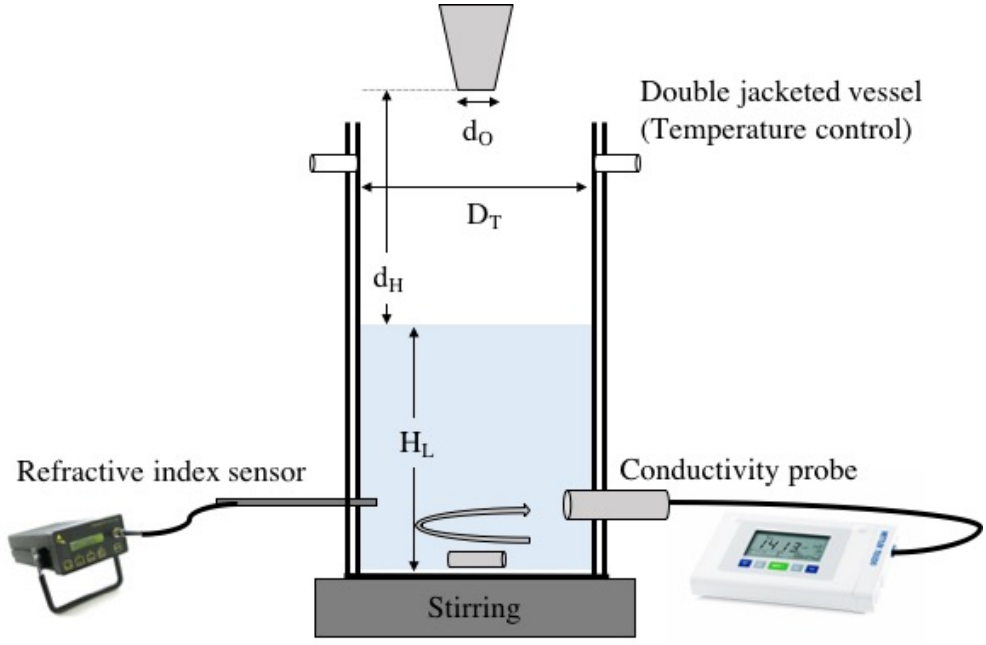

Figure 1. Experimental set-up to quantify powder dissolution, with control of temperature and stirring speed.

Powders were poured from funnels with different orifice diameters, d_O, of 7, 10, 12 and 15 mm, in order to vary the powder addition rate. The experiments involved feeding either 12.8 or 40 g of the powder into 160 or 500 mL of Évian mineral water at either 22 or 70 ℃ (i.e., leading to a final concentration of suspended solid of 7.41 wt%). The stirrer bar was rotated at 100 or 500 rpm and the funnel orifice was positioned at a constant height of 11 cm above the static liquid surface (d_H).

All experiments were repeated at least three times. Occasionally, the magnetic stirrer was affected by the powder inflow, leading to the error in conductivity measurements.

The entire powder rehydration process was also monitored using a Basler camera with a resolution of 2.3 MP (acA1929-155 μm) allowing a qualitative visual evaluation of the dissolution process at the end of the first five minutes of each experiment. This qualitative rate-limiting regime mapping approach was previously carried out by Mitchell et al. [12] and Fitzpatrick et al. [4,20]. The terminology used by these workers to describe any rate limitations included: *sedimentation* (powder remaining at the bottom of the vessel); *air entrainment* (air bubbles entrained in the powder bed); *floating* (powder floating at the liquid surface); or *lumps* (powder lumps formed during the dispersion process). This approach only worked for powders that are able to dissolve and produce a transparent solution at the end of the experiment. Hence, in the present work it is only suitable to identify limiting regime maps for maltodextrins, but not for the milk powders.

3. RESULTS AND DISCUSSION

Owing to limited powder availability, the smaller vessel was used in experiments on the effects of water activity and liquid temperature.

3.1 Effect of a_w and liquid temperature on dissolution kinetics

This section highlights the important role of glass transition temperature, T_g, in relation to the moisture content of the powder on the wetting, clumping, dispersion and dissolution behavior of maltodextrins DE2 and DE21. It will also examine the rehydration of powders with controlled a_w at liquid temperatures of 22 and 70 °C and an orifice diameter of 10 mm. In Table 4 are summarized the addition rates of powders for different values of a_w.

Table 4: Addition rates of the powders with different a_w.

Powder	*dm*/*dt* (g/s) when $a_w = 0.22$	*dm*/*dt* (g/s) when $a_w = 0.33$	*dm*/*dt* (g/s) when $a_w = 0.43$	*dm*/*dt* (g/s) when $a_w = 0.49$
DE21	2.4 ± 0.2	2.1 ± 0.2	1.8 ± 0.1	1.3 ± 0.7
DE2	2.6 ± 0.3	2.6 ± 0.4	2.5 ± 0.1	2.2 ± 0.2

As can be seen from Table 4, the powder addition rate decreases as a_w increases (and the moisture content increases). The addition rates obtained for both DE21 and DE2 powders are consistent with the experimental results by Descamps et al. [23], who focussed on the flowability of DE21 as a_w is varied. These data indicate that at the higher moisture contents, the grains become more cohesive, leading to a decrease in powder flowability.

The T_g values for different moisture contents of DE2 and DE21 powders given in Table 2 indicate that T_g decreases noticeably as moisture content increases. T_g values have previously been successfully predicted using the Gordon and Taylor equation [24]:

$$T_g = \frac{w_1 \cdot T_{g1} + b w_2 \cdot T_{g2}}{w_1 + b w_2} \qquad (2)$$

where w_1 and w_2 are the weight fractions of water and powder sample, respectively, T_{g1} and T_{g2} are the respective glass transition temperatures in pure water and the dry powders, and b is a fitting parameter. The glass transition temperature of water, T_{g1} was considered to be -135 ℃ [25].

3.1.1 Maltodextrin DE2

Figure 2 shows the dissolution behavior for a range of controlled a_w DE2 samples at ambient temperature. The kinetic curves shown in Figure 2a are seen to be similar over the first 25 seconds, although depending on T_g (a_w), the extent of dissolution differs at longer times. The Gordon-Taylor fitting parameters (Eq. 2) were found to show good agreement with the experimental data (T_{g2} =

132.4 °C, b = 0.3102 and R^2 = 0.9951). The T_g values obtained here are consistent with the experimental results by Avaltroni et al. [26] and Smann et al. [27].

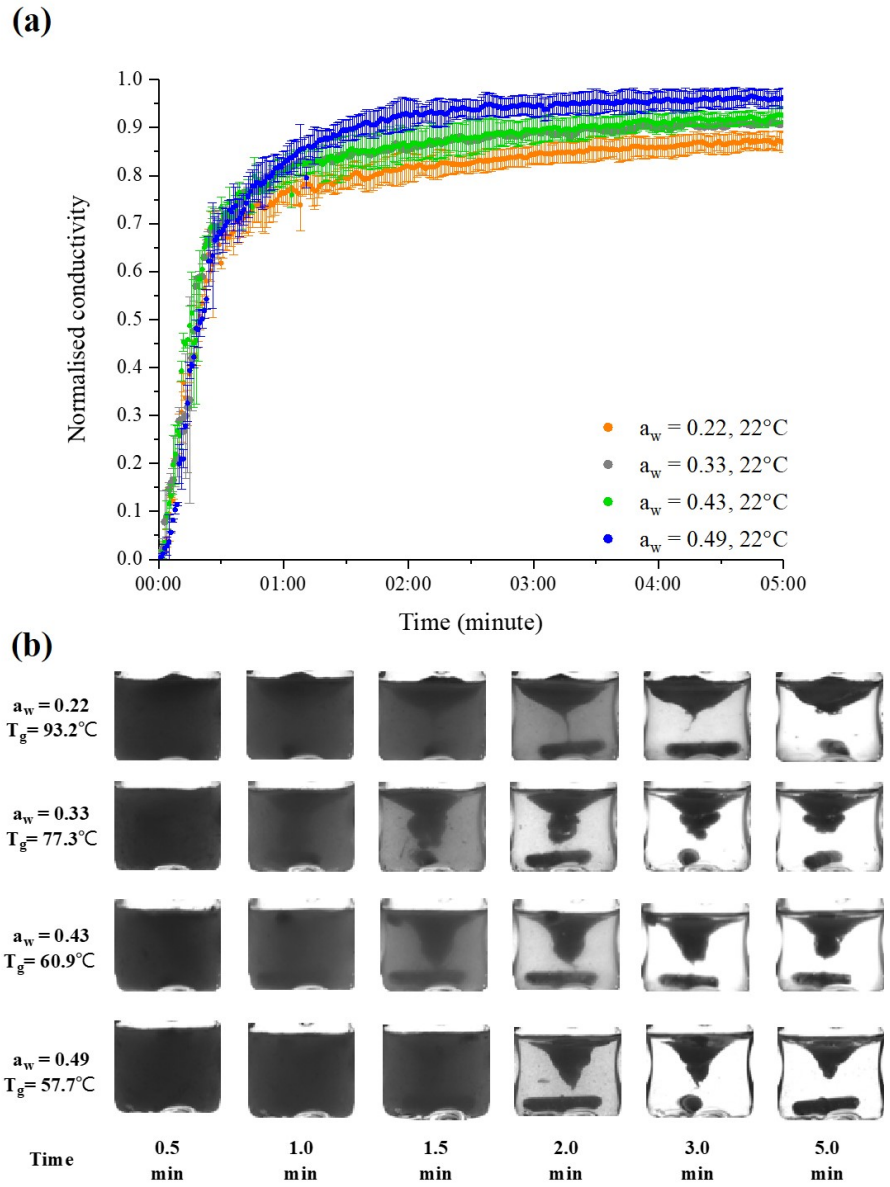

Figure 2. The dissolution behaviour of DE2 with different a_w in the small dissolution vessel at 500 rpm and 22 °C: (a) kinetic curves; (b) visual assessment with time.

199 Figure 3 shows the dissolution behavior for controlled a_w DE2 samples at 70 ℃. These results
200 show that the kinetics of dissolution are similar at 70 ℃ and 22 ℃ at $a_w = 0.49$ (compare Figures
201 3a and 2a). On the other hand, the results for lower a_w values contradict the previous literature [19]
202 inasmuch as there are significant differences at the two temperatures. Thus, it is seen in Figure 3b
203 that the sizes of the dispersed powder lumps for $a_w = 0.22$, 0.33 and 0.43 at 70 ℃ appear to be
204 larger than the corresponding ambient temperature system, shown in Figure 2b.
205 By comparing the data given in Figures 2a and 3a, the normalised conductivity for a range of
206 controlled a_w DE2 powders at 22 and 70 °C can be seen to be similar over the first ten seconds,
207 but diverged thereafter. This suggests that the initial wetting is similar at the two temperatures, but
208 also that opposing effects are occurring at longer times. It is possible that diffusion of water into a
209 powder grain is inhibited under certain temperature conditions, as a result of specific surface
210 interactions taking place. Deslandes et al. [28], for example, observed that starch granules swell in
211 water between 62 – 74 °C, indicating a sensitivity to hydration of the polymeric carbohydrate
212 within this temperature range. In the present systems, at the higher temperature studied,
213 competition between the rates of dispersion and of the onset of hydration, might favour the latter
214 to occur preferentially, such that the grains become partially hydrated, with a T_g below the liquid
215 temperature, and hence 'sticky', leading to agglomeration. Conversely, at 22 °C, the temperature
216 is below the T_g and grains have more time to disperse before agglomeration occurs [19]. This
217 suggests that the relationship between the liquid temperature and T_g could be studied further by
218 using a larger range of liquid temperatures.
219 Apart from the effect of T_g, the contact angle (i.e. wettability) and the change in viscosity of the
220 grain surfaces could be the mechanism responsible for delaying the reconstitution of DE 2 at high

liquid temperature. This could be studied further in a quantitative manner by determining the contact angle of different food powders as a function of initial a_w [29].

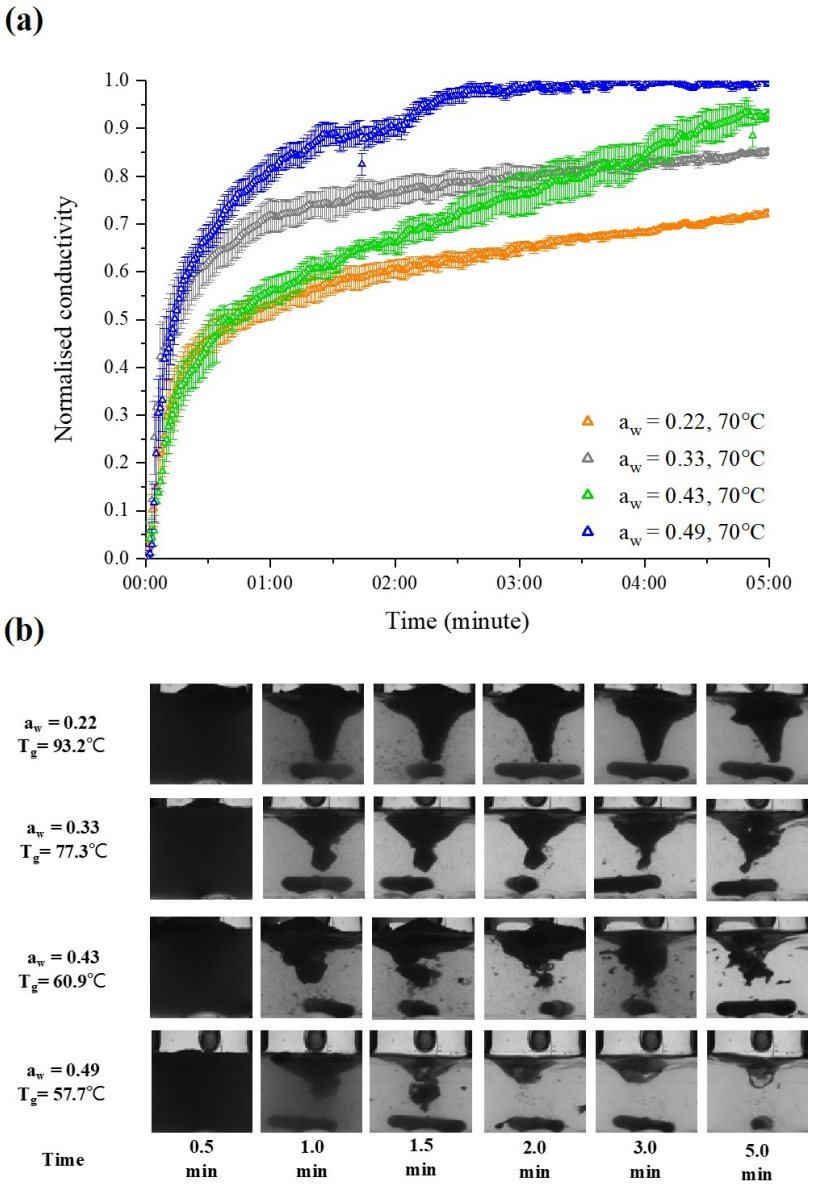

Figure 3. The dissolution behaviour of DE2 with different a_w in the small vessel at 500 rpm and 70 °C: (a) kinetic curves; (b) visual assessment with time.

228 3.1.2 Maltodextrin DE21

229 The influence of water activity on the dissolution kinetics of DE21 is shown in Figure 4. In this
230 case, it is found that the dissolution at 22 °C improved when T_g decreases (and a_w increases).
231 Additionally, as expected, the overall dissolution time was found to be shorter at the higher liquid
232 temperature. At 70 °C (close to T_g), however, the effect of a_w on the dissolution time was not
233 measurable, being too rapid. Hence, the dissolution of controlled a_w DE21 powders in the range
234 0.22 – 0.49 are similar. At ambient temperature, lumps containing entrapped air were evident in
235 the solution (inset in 4a), whereas at high temperature this was not observed. The Gordon-Taylor
236 fitting parameters (Eq. 2) were found to show reasonable agreement with the experimental data
237 (T_{g2} = 94.6 °C, b = 0.5536 and R^2 = 0.9876) and comparable with those of Descamps et al. [23].

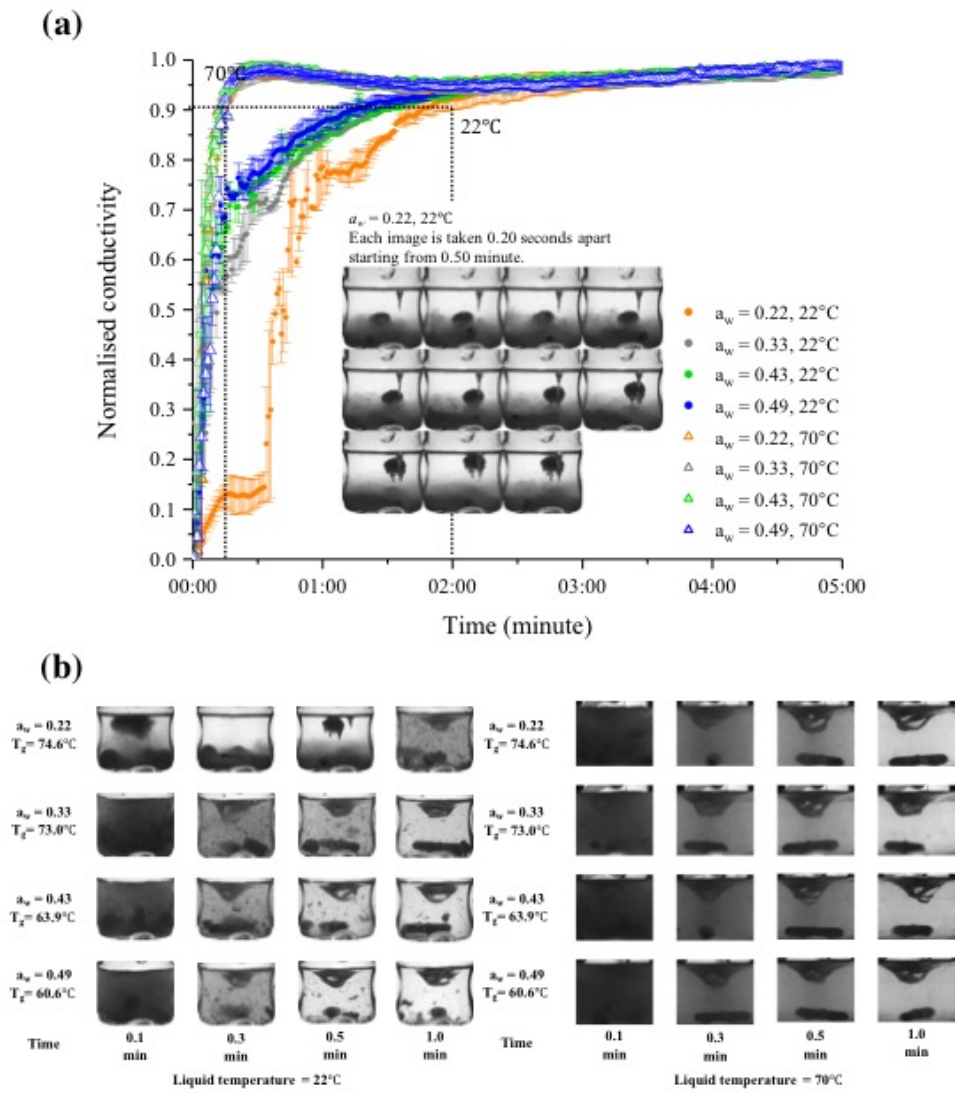

238

239 **Figure 4.** The dissolution behavior of DE21 with different a_w in the small vessel at 500 rpm, at 22 and 70

240 °C: (a) kinetic curves (the inset shows lumps containing entrapped air in the solution); (b) visual assessment

241 with time.

242 3.2 Effect of vessel design on dissolution kinetics

243 To investigate the effects of vessel design on powder dissolution, two different double-jacketed

244 vessels were used, with the dimensions for each being given in Table 3.

245 Figure 5 compares the normalized conductivity curves of DE21 and DE2 in both small and large

246 vessels. With a constant addition rate of 1.39 g/s, within experimental error, the normalised

247 conductivity of DE21 is seen to be very similar for both vessels. The only difference to be noted
248 is that the dissolution kinetics of DE21 appears to be slightly slower in the large vessel over the
249 first 30 seconds.

250 On the other hand, at a constant addition rate of 2.78 g/s, there was a significant discrepancy in
251 the dissolution behaviour of DE2 between the two vessels. As seen in Figure 5, the normalized
252 conductivity in the small vessel was almost 1.5 times higher than the large vessel after five minutes.
253 In this example, the powder concentration was constant in both vessels, for which the aspect ratio
254 differed by 1.5×, as given in Table 3. The lower dissolution of DE2 in the large vessel can therefore
255 be explained in terms of the lower surface area per unit volume in the large vessel which reinforces
256 the tendency for DE2 to float on the liquid surface. On the basis of the sensitivity shown by DE2
257 in the large vessel, we chose to use this system in subsequent experiments to elucidate the effects
258 of powder addition rate and agitation speed.

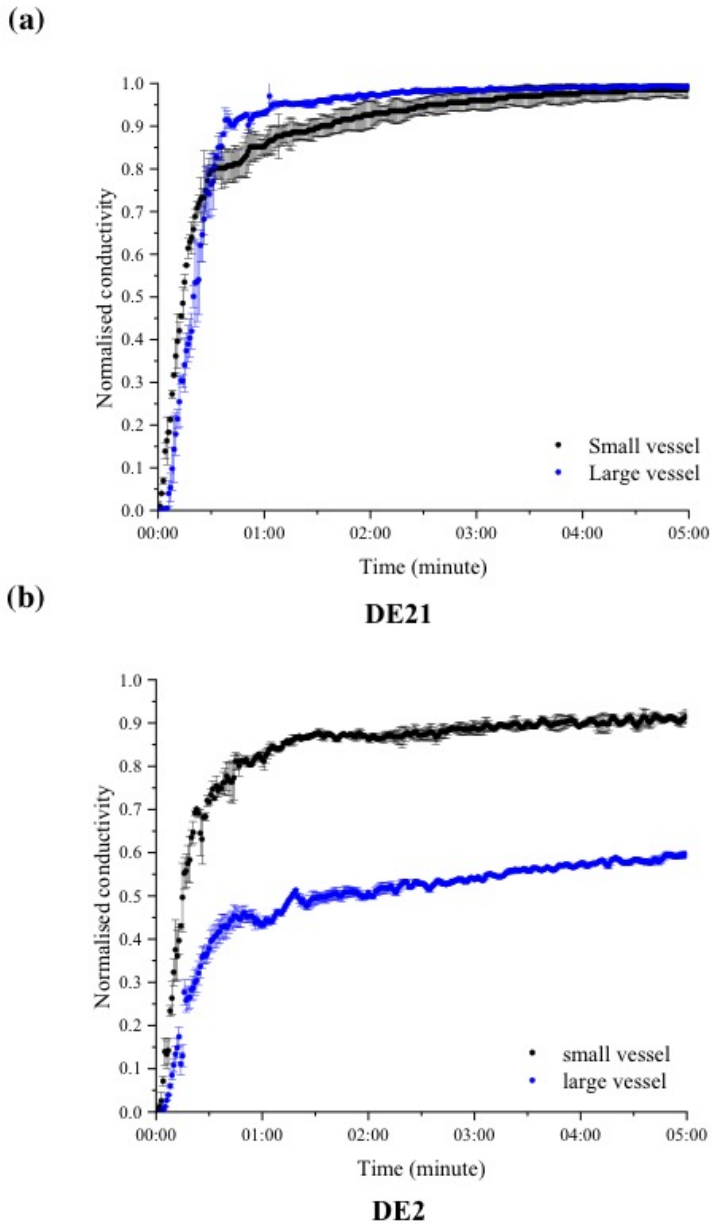

259

260 **Figure 5.** Dissolution kinetics for DE21 (a) and DE2 (b) in the large and small vessels at 500 rpm, 22 °C.

261

262 3.3. Effect of powder addition rate on dissolution kinetics

263 Two different liquid stirring speeds were considered: (a) 100 rpm, to provide some degree of
264 mixing within the cell, while maintaining a flat liquid interface and avoiding the formation of a
265 central vortex; and (b) 500 rpm, leading to the formation of a central vortex.

3.3.1 Maltodextrin DE2

The effect of powder addition rate on the reconstitution kinetics of DE2 is shown in Figures 6 (at 100 rpm) and 7 (at 500 rpm). The lateral snapshot included in these figures show that DE2 floated at the liquid interface owing to the higher contact angle and the reconstitution was incomplete after five minutes.

At low liquid agitation (100 rpm, Figure 6), and using a smaller funnel for powder addition, to produce a lower powder addition rate, the reconstitution was found to be faster and more complete. Increasing the liquid agitation speed to 500 rpm (Figure 7) further improved reconstitution, compared with 100 rpm, although under these conditions the reconstitution was never found to be complete.

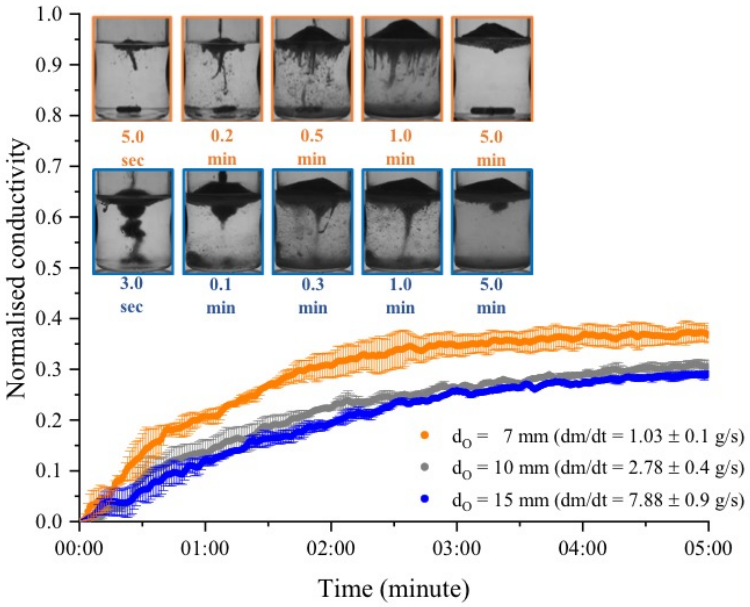

Figure 6. DE2 reconstitution kinetics at 100 rpm. Different colours represent different powder addition rates onto the liquid. The colored outlines around the inset lateral images taken during the reconstitution experiments refer to the kinetic curves.

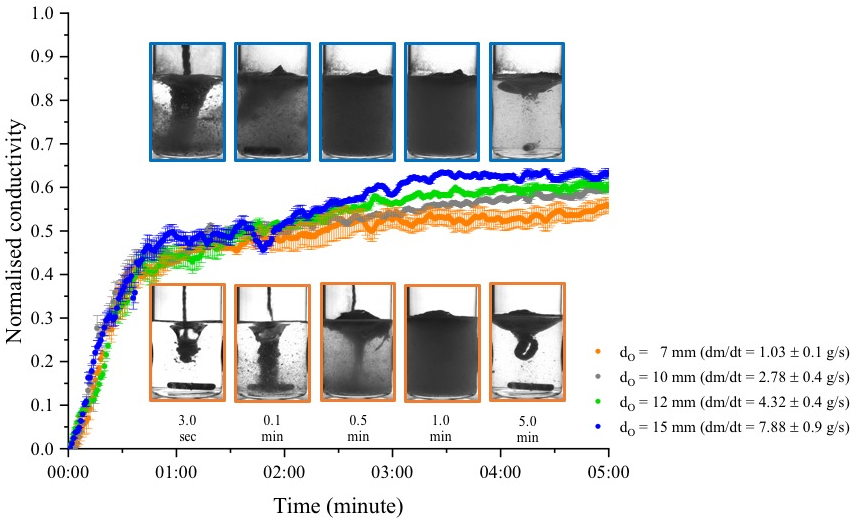

Figure 7. DE2 reconstitution kinetics at 500 rpm. Different colours represent different powder addition rates onto the liquid. The colored outlines around the inset lateral images taken during the reconstitution experiments refer to the kinetic curves.

Due to the high molecular weight of DE2 [17], the dissolution of individual grains may result in a local viscosity increase and pore collapse, preventing water from wicking into the inter- and intra-particle voids of the floating powder layer [30]. A large number of air bubbles can be seen in Figure 6. By de-gassing the mineral water under vacuum before conducting the experiments, it was verified that the bubbles did not originate from air initially dissolved in water. Rather, the air is originally entrained in the water with the powder grains; the bubbles adhering to the powder grains then coalesce, becoming more obvious throughout the rehydration process.

When a poorer wettability causes retention of the grains at the interface, a powder island forms, as studied quantitatively by Raux et al. [2] and Ong et al. [3]. The dispersion of grains into the liquid upon impacting the interface is favored by their kinetic energy and is limited by the local energy barriers that the liquid encounters when wicking into the grain pores. The effect of DE2 addition rate on reconstitution rate at 100 rpm (Figure 6) is particularly strong in the first minute.

298 Indeed, when a low powder addition rate is used, the powder island grows slowly, and grains are
299 able to overcome the local energy barriers and disperse at a rate comparable to their addition rate,
300 as a result of their kinetic energy. For higher powder addition rates, the grains accumulate quickly
301 over the whole liquid interface, and further added grains impinge on the surface grains, thus
302 dissipating the kinetic energy in the resulting grain-grain impacts.
303 At the higher agitation speed (500 rpm, Figure 7), the central vortex is able to promote the
304 sinking of the grains by lowering the energy barriers during wicking due to the higher pressure
305 difference across the liquid interface [2]. This slows down the accumulation of grains and increases
306 strongly the reconstitution kinetics. Thus, the dissolution kinetics of DE2 at the higher addition
307 rate were found to be faster than at the lower addition rate after five minutes (as shown in Figure
308 7). These results oppose the previous results for lower agitation speed, for which at low addition
309 rate (low grain kinetic energy) the grains are more likely to float without deforming the interface.
310 This explains the observed retention of grains at the interface shown in Figure 7 as seen in the inset
311 image (orange outline at 0.50 minutes). With the assistance of the vortex, powder impacting at
312 high addition rate tends to sink instead of being retained at the interface, thereby improving the
313 efficiency of powder hydration.
314
315 3.3.2. Maltodextrin DE21
316 The results presented in Figure 8 show that DE21 reconstitution was very slow and incomplete
317 at low agitation speed (100 rpm), even after five minutes. Furthermore, the powder addition rate
318 had a minor and insignificant effect on the kinetics of reconstitution under these conditions. At
319 both addition rates, the powder sank rapidly and sedimented to the bottom of the cell.
320

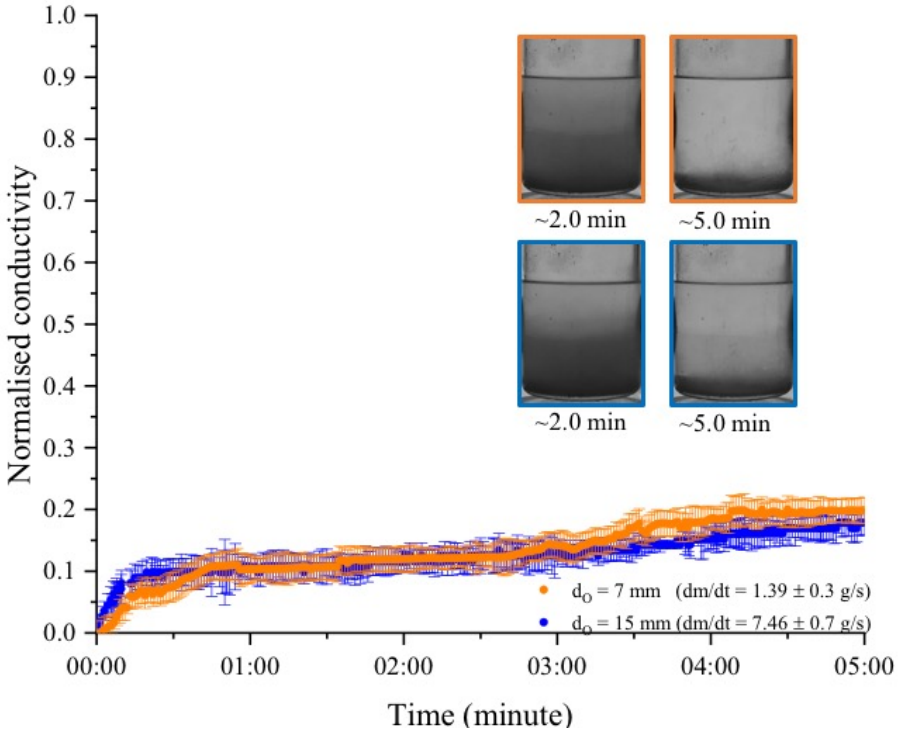

Figure 8. Dissolution DE21 reconstitution kinetics at 100 rpm. Different colors represent different powder addition rates onto the liquid. On the right hand side are reported lateral images taken during the reconstitution experiments. The inset images shown in each graph were highlighted based on the colors of the kinetic curves.

Conversely, Figure 9 shows that at high agitation speed (500 rpm) the reconstitution was almost complete after only one minute. The powder addition rate had a measurable effect on the reconstitution kinetics within the first minute. As in the previous case, DE21 sank very rapidly and the lower signal measured initially at low addition rate is a consequence of the smaller amount of maltodextrin present in the cell.

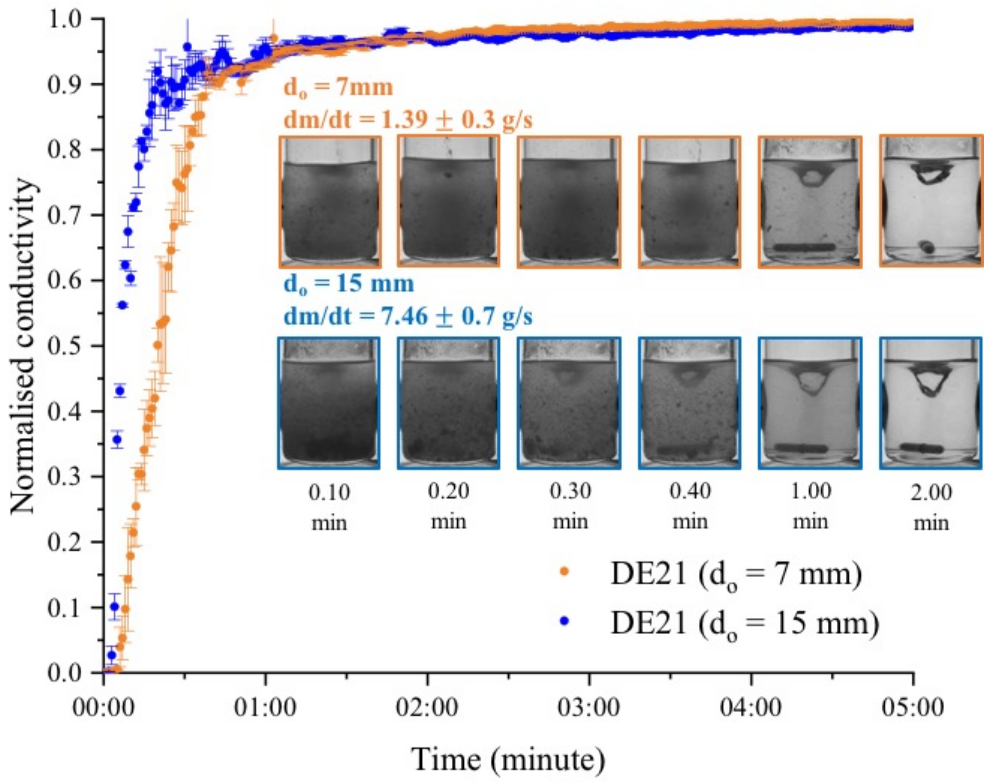

335

336 **Figure 9.** DE21 reconstitution kinetics at 500 rpm. Different colours represent different powder addition
337 rates onto the liquid. Inset are shown lateral images taken during the reconstitution experiments, the outline
338 colors refer to the kinetic curves.

339

340 The results reported above can be interpreted considering the different mechanisms occurring
341 during the reconstitution process. When grain wettability is good, such as for DE21, powder grains
342 readily enter the liquid interface and sediment due to their higher density. If the liquid agitation is
343 insufficient to maintain the grains in suspension, they sediment to the bottom of the vessel, forming
344 a region of higher concentration that further limits the mixing efficiency. The powder addition rate
345 has therefore a negligible impact on reconstitution.

346 3.4. Improving powder distribution in a liquid: A novel powder distributor

In a vessel agitated by a stirrer, such as the one used in this study, the liquid is convected upwards at the vessel walls and downwards at the center. This results in an inward radial flow at the surface of the liquid, therefore powder grains fed into the center of the vessel which float are seen to accumulate rapidly to create an island.

In order to avoid the powder grains accumulating on the liquid surface at the point of impact, a novel, yet simple, powder distributor has been developed as part of this study. This is depicted in Figure 10. The distributor is positioned over the liquid surface and serves to distribute the powder grains poured from the funnel towards the vessel walls.

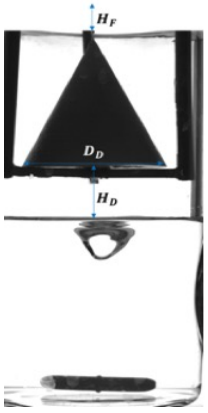

Height of funnel from the distributor, H_F (cm)	Distributor height over the liquid, H_D (cm)	Distributor diameter, D_D (cm)
2.5	2.5	6

Figure 10. Experimental set-up to quantify the effect of the novel conical powder distributor in facilitating the dispersion and dissolution processes in the large vessel.

The dissolution curves shown in Figure 11 demonstrate the strong improvement in powder reconstitution obtained using this simple arrangement. It can be seen in Figure 11a, for example, that there is rapid and almost complete dissolution of DE2 powder in the first 20 seconds with the assistance of the distributor. In the absence of the distributor, DE2 experienced much slower dissolution where the normalized conductivity was only 50% during the first minute, and over the next nine minutes the value only increased to 63%. As described above, this is a likely consequence

365 of the reduced diffusion of water into the bulk of the grains due to the presence of a less-permeable
366 surface layer.

367 On the other hand, no measurable effect was obtained when using this powder distributor with
368 DE21, due to the good wettability of the powder and the absence of powder accumulation at the
369 water interface. However, measurable improvements in the reconstitution kinetics have been found
370 when using the distributor with commercial food powders which initially float at the surface.

371 For WMP and Horlicks, respectively, Figure 11b and 11c show the normalized conductivities to
372 be >50% higher with the distributor at the end of the experiments.

373 Thus, instead of applying the powder to the center of the vessel, the distributor allows the powder
374 to fall towards the side walls. The inwards surface flow then moves the grains away from the wall,
375 liberating the air-liquid interface for new grains. By avoiding grain-grain contacts at the liquid
376 surface, a higher proportion of the kinetic energy of the grains is available to facilitate them to pass
377 into the bulk of the liquid.

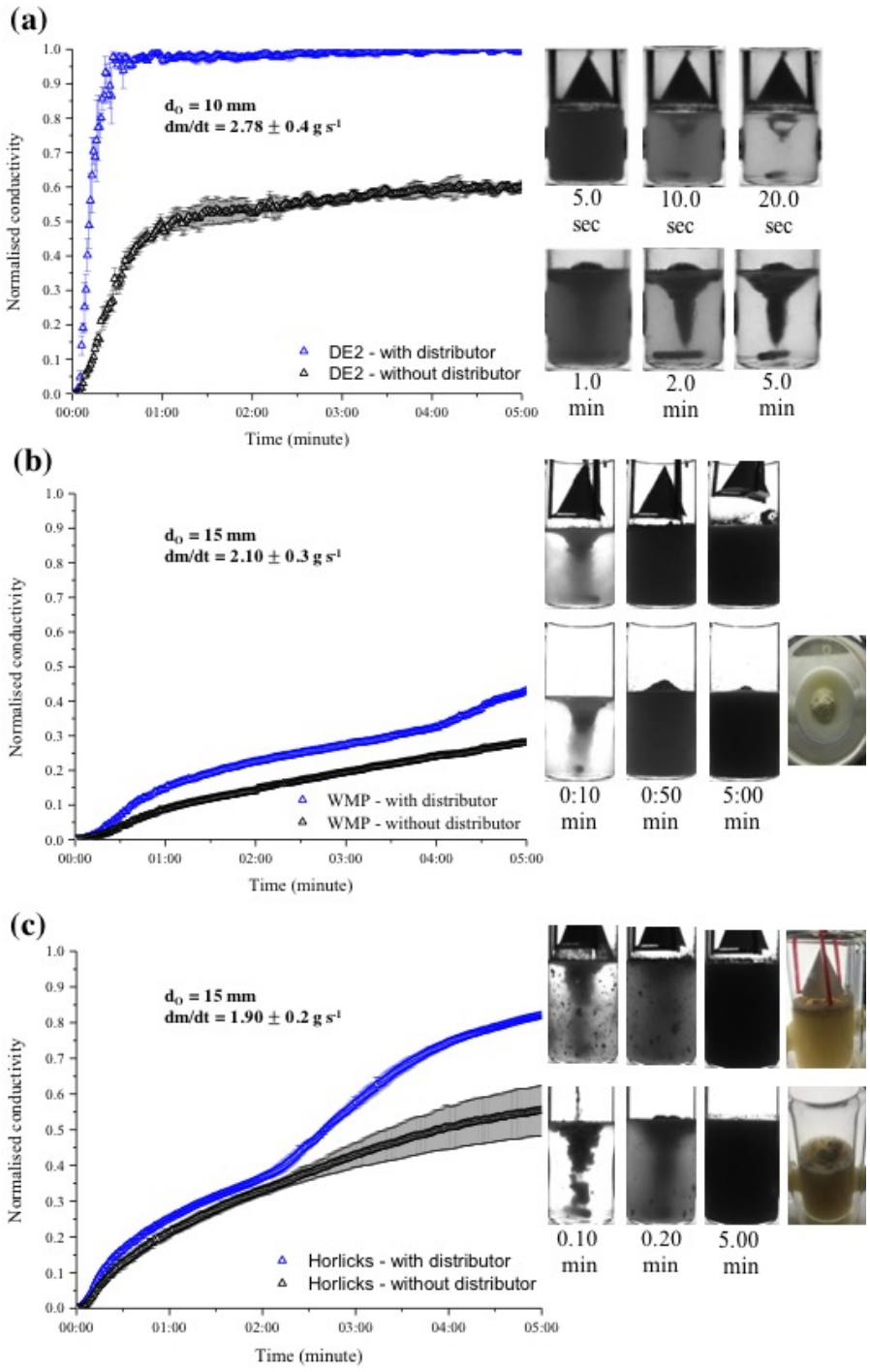

Figure 11. Comparison of the dissolution kinetics of different types of food powder with and without the distributor in the large vessels at 500 rpm and 22 ℃: (a) DE2, (b) WMP and (c) Horlicks.

4. CONCLUSIONS

The complex interplay of powder properties and process conditions, such as liquid temperature and agitation speed, on the reconstitution of maltodextrins has been studied in the present paper. This serves to highlight some of the limitations on powder dispersion arising from the formation of powder islands at the water interface. In general, an increase in agitation speed and liquid temperature improved the rehydration performance of the food powders studied, but depending on the other physical properties, the way in which these variables influence the rehydration process can differ. Mixing helped to reduce sedimentation of short-chained maltodextrin powders (DE21). Higher liquid temperatures improved the dissolution of lower molecular weight carbohydrates (DE21) but worsened the dispersion of carbohydrates with higher molecular weight (DE2). This finding is possibly a consequence of the liquid temperature (70 °C) not being high enough to promote fast dispersion before the formation of sticky layers around the grains, leading to agglomeration, whereas at lower liquid temperature (below the T_g), DE2 grains have more time to disperse. Powder addition rate can also have opposing effects on reconstitution kinetics depending on the liquid agitation speed. We have demonstrated that a novel, simple powder distributor can significantly improve the reconstitution of powders with a tendency to float at the liquid surface, by limiting grain-grain contacts which dissipate the kinetic energy. It is anticipated that such a demonstration should lead to an improved understanding of the reconstitution of food product formulations, food processing and the design of powdered food products. Interesting directions for future investigation include studying systematically the inter-relationship between water activity, glass transition temperature, contact angle and viscosity of different food powders. This approach would allow the effect of grain swelling, and the formation of surface gels to be evaluated, which would provide guidelines towards improving powder dispersion and dissolution.

405

406 AUTHOR INFORMATION

407 ***Corresponding Author**

408 E-mail: x.ong@surrey.ac.uk (X.Y. Ong)

409 **Notes**

410 The authors declare no competing financial interest.

411 ACKNOWLEDGMENT

412 This work was supported by funds from the Chemical and Process Engineering Department of
413 the University of Surrey.

414 **REFERENCES**

415 [1] S. V. Crowley, A.L. Kelly, P. Schuck, R. Jeantet, J.A. O'Mahony, J.A. O Mahony,
416 Rehydration and solubility characteristics of high-protein dairy powders, in: Adv. Dairy
417 Chem. Vol. 1B Proteins Appl. Asp. Fourth Ed., Springer New York, New York, NY, **2016**:
418 pp. 99–131.

419 [2] P.S. Raux, H. Cockenpot, M. Ramaioli, D. Quéré, C. Clanet, Wicking in a powder,
420 *Langmuir*. 29 (**2013**) 3636–3644.

421 [3] X.Y. Ong, S.E. Taylor, M. Ramaioli, Pouring of Grains onto Liquid Surfaces: Dispersion
422 or Lump Formation?, *Langmuir*. (**2019**).

423 [4] J.J. Fitzpatrick, A. van Lauwe, M. Coursol, A. O'Brien, K.L. Fitzpatrick, J. Ji, S. Miao,
424 Investigation of the rehydration behaviour of food powders by comparing the behaviour of

twelve powders with different properties, *Powder Technol*. 297 (**2016**) 340–348.

[5] F. Lequeux, L. Talini, E. Verneuil, G. Delannoy, P. Valois, Wetting of polymers by their solvents, *Eur. Phys. J. E. Soft Matter*. 39 (**2016**) 12.

[6] J. Dupas, E. Verneuil, M. Ramaioli, L. Forny, L. Talini, F. Lequeux, Dynamic wetting on a thin film of soluble polymer: Effects of nonlinearities in the sorption isotherm, *Langmuir*. 29 (**2013**) 12572–12578.

[7] J. Dupas, E. Verneuil, M. Van Landeghem, B. Bresson, L. Forny, M. Ramaioli, F. Lequeux, L. Talini, Glass transition accelerates the spreading of polar solvents on a soluble polymer, *Phys. Rev. Lett*. 112 (**2014**) 188302.

[8] R.G. Cox, The dynamics of the spreading of liquids on a solid surface. Part 2. Surfactants, *J. Fluid Mech*. 168 (**1986**) 195–220.

[9] O. V. Voinov, Hydrodynamics of wetting, *Fluid Dyn*. 11 (**1976**) 714–721.

[10] L. Galet, T.O. Vu, D. Oulahna, J. Fages, The wetting behaviour and dispersion rate of cocoa powder in water, *Food Bioprod. Process*. 82 (**2004**) 298–303.

[11] B. Freudig, S. Hogekamp, H. Schubert, Dispersion of powders in liquids in a stirred vessel, *Chem. Eng. Process. Process Intensif*. 38 (**1999**) 525–532.

[12] W.R. Mitchell, L. Forny, T.O. Althaus, G. Niederreiter, S. Palzer, M.J. Hounslow, A.D. Salman, Mapping the rate-limiting regimes of food powder reconstitution in a standard mixing vessel, *Powder Technol*. 270 (**2015**) 520–527.

[13] J. Ji, K. Cronin, J. Fitzpatrick, M. Fenelon, S. Miao, Effects of fluid bed agglomeration on

the structure modification and reconstitution behaviour of milk protein isolate powders, *J. Food Eng*. 167 (**2015**) 175–182.

[14] J. Ji, K. Cronin, J. Fitzpatrick, S. Miao, Enhanced wetting behaviours of whey protein isolate powder: The different effects of lecithin addition by fluidised bed agglomeration and coating processes, *Food Hydrocoll*. 71 (**2017**) 94–101.

[15] J. Ji, J. Fitzpatrick, K. Cronin, A. Crean, S. Miao, Assessment of measurement characteristics for rehydration of milk protein based powders, *Food Hydrocoll*. 54 (**2016**) 151–161.

[16] J. Ji, J. Fitzpatrick, K. Cronin, P. Maguire, H. Zhang, S. Miao, Rehydration behaviours of high protein dairy powders: The influence of agglomeration on wettability, dispersibility and solubility, *Food Hydrocoll*. 58 (**2016**) 194–203.

[17] J. Dupas, Wetting of soluble polymers, **2012**.

[18] J. Burgain, J. Scher, J. Petit, G. Francius, C. Gaiani, Links between particle surface hardening and rehydration impairment during micellar casein powder storage, *Food Hydrocoll*. 61 (**2016**) 277–285.

[19] J. Dupas, V. Girard, L. Forny, Reconstitution properties of sucrose and maltodextrins, *Langmuir*. 33 (**2017**) 988–995.

[20] J.J. Fitzpatrick, J. Salmon, J. Ji, S. Miao, Characterisation of the wetting behaviour of poor wetting food powders and the influence of temperature and film formation, *KONA Powder Part. J*. 34 (**2017**) 282–289.

[21] Y. Rong, M. Sillick, C.M. Gregson, Determination of dextrose equivalent value and number average molecular weight of maltodextrin by osmometry, *J. Food Sci.* 74 (**2009**) C33–C40.

[22] W.R. Mitchell, L. Forny, T. Althaus, D. Dopfer, G. Niederreiter, S. Palzer, Compaction of food powders: The influence of material properties and process parameters on product structure, strength, and dissolution, *Chem. Eng. Sci.* 167 (**2017**) 29–41.

[23] N. Descamps, S. Palzer, Y.H. Roos, J.J. Fitzpatrick, Glass transition and flowability/caking behaviour of maltodextrin DE 21, *J. Food Eng.* 119 (**2013**) 809–813.

[24] M. Gordon, J.S. Taylor, Ideal copolymers and the second-order transitions of synthetic rubbers. i. non-crystalline copolymers, *J. Appl. Chem.* 2 (**1952**) 493–500.

[25] G.P. Johari, A. Hallbrucker, E. Mayer, The glass-liquid transition of hyperquenched water, *Nature*. 330 (**1987**) 552–553.

[26] F. Avaltroni, P.E. Bouquerand, V. NORMAND, Maltodextrin molecular weight distribution influence on the glass transition temperature and viscosity in aqueous solutions, *Carbohydr. Polym.* 58 (**2004**) 323–334.

[27] R.G.M. Van Der Sman, M.B.J. Meinders, Prediction of the state diagram of starch water mixtures using the Flory-Huggins free volume theory, *Soft Matter*. 7 (**2011**) 429–442.

[28] F. Deslandes, A. Plana-Fattori, G. Almeida, G. Moulin, C. Doursat, D. Flick, Estimation of individual starch granule swelling under hydro-thermal treatment, *Food Struct.* 22 (**2019**) 100125.

[29] J. Dupas, L. Forny, M. Ramaioli, Powder wettability at a static air–water interface, *J.*

Colloid Interface Sci. 448 (**2015**) 51–56.

[30] L. Forny, A. Marabi, S. Palzer, Wetting, disintegration and dissolution of agglomerated water soluble powders, *Powder Technol*. 206 (**2011**) 72–78.

APPENDIX A

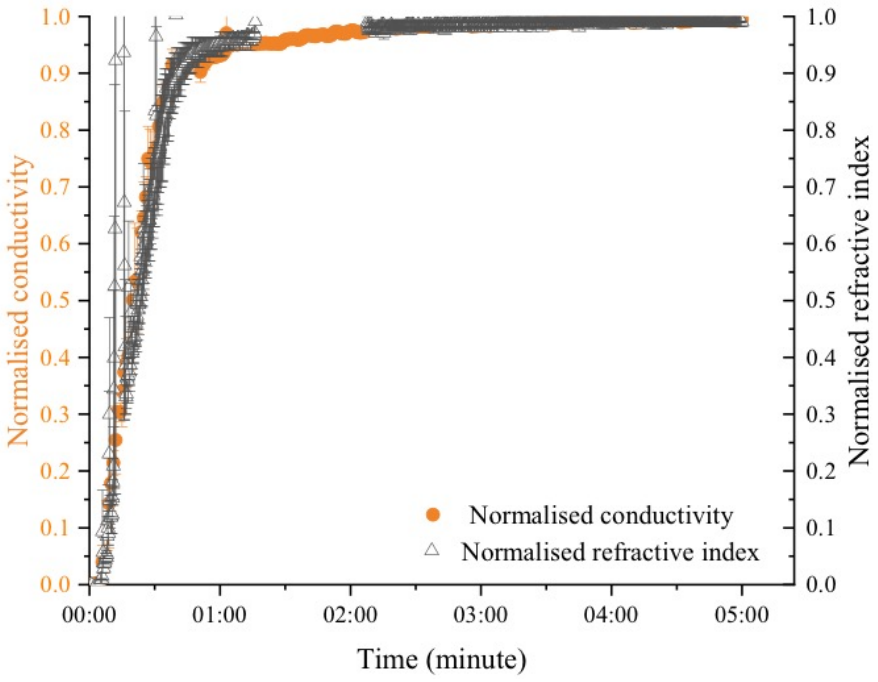

Figure A1. DE21 reconstitution kinetics at 500 rpm, 22 ℃. The orifice diameter, d_O of 7 mm was used to obtain the powder addition rate of 1.39 g/s. The comparison of normalised dissolution index between the conductivity (orange) and the refractive index (black) reading.